ADNI Alzheimer's Disease Neuroimaging Initiative

Flortaucipir (AV-1451) processing methods

Susan Landau, Alice E. Murphy, Jia Qie Lee, Tyler J. Ward, & William Jagust
Helen Wills Neuroscience Institute, UC Berkeley and Lawrence Berkeley National Laboratory

Summary

ADNI ^{18}F flortaucipir regional summary data are updated regularly and uploaded to LONI by our group. Our image analysis pipeline includes one or more flortaucipir scans, paired with one or more structural MRI scans, for each subject. The available MRI that is closest in time to each PET is segmented with Freesurfer (version 7.1.1) to define regions of interest in native space. We then coregister each flortaucipir scan to its corresponding bias-corrected T1 created by Freesurfer and compute the mean flortaucipir uptake within each region. **Flortaucipir SUVRs can be generated using the UC Berkeley dataset using a single region of interest or averaging across several regions of interest (e.g. Braak stage composite regions – see below) and dividing by a reference region such as inferior cerebellar GM (see details below) or hemispheric WM .**

Version Information

This document supersedes our previous document dated 01-14-2021. In previously uploaded datasets, we have defined regions for baseline and subsequent PET using the MRI scan *closest in time to the first* flortaucipir scan. Starting with the November 2021 dataset, non-timepoint specific (NONTP) PET-MRI pairing has been updated to a timepoint specific (TP) method, where we use the MRI scan *closest in time to each* flortaucipir scan.

The figure below shows the effect of this timepoint-specific MRI selection on longitudinal SUVRs across ADNI flortaucipir visits. Note that *baseline* PET SUVRs are identical across the NONTP and TP datasets.

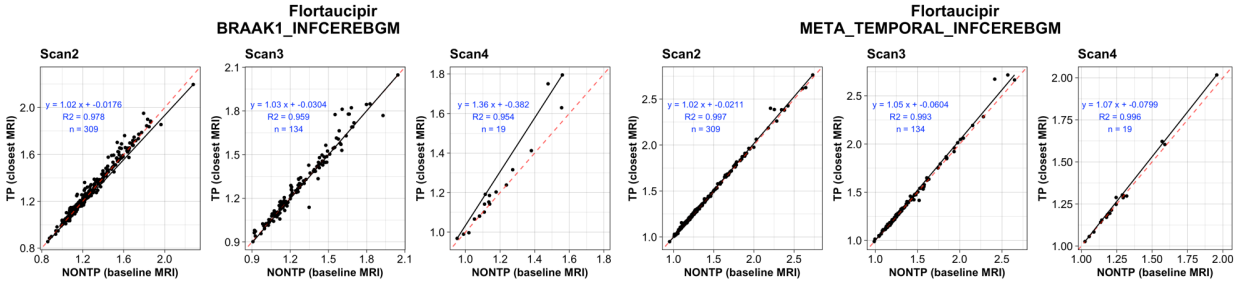

The November 2021 flortaucipir partial volume corrected dataset is processed with the MRI scan that is closest in time to **baseline** flortaucipir.

Are the flortaucipir data in our dataset already intensity normalized?

Yes. Regional flortaucipir means in our dataset are SUVRs that have already been intensity normalized by Bob Koeppe during the generation of the pre-processed images available for download from LONI. The Stage 3 flortaucipir images as well as the Stage 4, fully pre-processed flortaucipir images ("AV1451 Coreg, Avg, Std Img and Vox Siz, Uniform Resolution") are SUVR images that have been *approximately* intensity normalized using an atlas-space cerebellar cortex region defined by Bob Koeppe during his pre-processing procedures (see Jagust et al. Alz & Dementia 2015 and PET preprocessing info at adni.loni.usc.edu). These procedures include defining an atlas-space cerebellar cortex region using a coregistered FDG or MPRAGE scan and reverse normalizing this region back onto the native space flortaucipir image. This initial intensity normalization carries with it some noise associated with the warping procedures, so we defined native-space reference regions (as well as regions of interest) more precisely using Freesurfer. We recommend replacing (e.g. dividing out) the initial intensity normalization carried out by Bob Koeppe with a subsequent intensity normalization using our Freesurfer-defined, native space reference regions.

However, we recommend intensity normalizing the regional SUVRs in our dataset using one of the reference regions in our dataset, since the initial intensity normalization applied during pre-processing did not take advantage of FreeSurfer-defined regional information.

In order to generate SUVRs that take advantage of our Freesurfer-based target and reference regions, divide a region of interest SUVR mean (e.g. Braak1) by one of the reference regions we provide in our dataset. The recommended reference region for cross-sectional flortaucipir is the inferior cerebellar reference region (variable name: INFERIORCEREBELLUM_SUVR; see details about region definition below).

Method

Acquisition of flortaucipir and MRI image data from LONI

We download flortaucipir data from LONI in the most fully pre-processed format (series description in LONI Advanced Search: "AV1451 Coreg, Avg, Std Img and Vox Siz, Uniform Resolution"). Each subject's pre-processed flortaucipir image is coregistered using SPM to that subject's MRI image (series description: ADNI 1 scans *N3;*, ADNI GO/2 scans *N3*, and ADNI 3 *Accel*) acquired closest in time to the first flortaucipir scan.

Calculation of flortaucipir SUVR

We have investigated a number of strategies for quantifying and staging tau using flortaucipir *[1-4]*. This ADNI UC Berkeley flortaucipir dataset includes a broad set of regional flortaucipir means and their corresponding Freesurfer-defined volumes (mm^3). This set includes cortical and subcortical regions of interest and reference regions such as inferior cerebellar grey matter and eroded hemispheric WM. We approximate uptake in the anatomical Braak stages [5] by calculating volume-weighted means of groups of FreeSurfer-defined regions, specified in the "Braak ROIs" section. Additionally, we include a meta-temporal region, composed of Freesurfer-defined bilateral entorhinal, amygdala, fusiform, inferior and middle temporal cortices, outlined in the "MetaTemporal ROI" section [8].

As described in the box above, flortaucipir SUVRs can be calculated by dividing a region of interest (with or without an adjustment for regional volume) by a reference region (e.g. inferior cerebellar grey matter; see below for more details).

Flortaucipir Partial Volume Correction

We also provide a separate dataset with flortaucipir SUVRs corrected for partial volume effects using the Geometric Transfer Matrix (GTM) approach [6] as implemented by Suzanne Baker [1,2]. The GTM approach we are currently using models all FreeSurfer-defined ROIs (see list below) as well as regions in which off-target binding is common (e.g. choroid plexus) in order to reduce contamination from these regions into neighboring regions of interest.

In order to reduce the influence of off-target flortaucipir binding that has been observed in the dorsal cerebellum, we defined an inferior cerebellar GM reference region using the SUIT template [7] (http://www.diedrichsenlab.org/imaging/suit.htm) (see below for more details) and reverse-normalized this region back to each subject's native space as described in Baker et al. NeuroImage 2017[2].

In our flortaucipir PVC and non-PVC datasets, we use the individual Freesurfer-defined SUVRs and volumes to calculate weighted averages of the following composite regions (Braak 1, Braak 3/4, Braak 5/6) that approximate the spread of tau as depicted by Braak and Braak [5] and described in Scholl et al. [4] and Maass et al [3]. **We include both Braak 1 (entorhinal) alone and Braak 1/2 (entorhinal and hippocampus) but we note that the hippocampus is known to be contaminated by off-target binding in the choroid plexus. It is unclear whether this can be adequately corrected by partial volume correction. Note, the PVC dataset uses the same MRI across baseline and subsequent flortaucipir scans, while the non-PVC dataset uses the MRI that is closest in time to each flortaucipir scan.**

We recommend normalizing either composite (e.g. Braak) or individual PVC ROI values by a PVCed reference region (e.g. inferior cerebellar grey matter; see below for more details).

Freesurfer-defined composite ROIs

Braak 1 and 2 composite region (Braak12):

Braak 1
1006 L_entorhinal
2006 R_entorhinal

Braak 2 (We have concluded that this region is contaminated by off-target binding in the choroid plexus and have eliminated it from most of our analyses although we have provided the data in our dataset)
17 L_hippocampus

53 R_hippocampus

Braak 3 and 4 composite region (Braak34):

Braak 3

1016 L_parahippocampal
1007 L_fusiform
1013 L_lingual
18 L_amygdala
2016 R_parahippocampal
2007 R_fusiform
2013 R_lingual
54 R_amygdala

Braak 4

1015 L_middletemporal
1002 L_caudantcing
1026 L_rostantcing
1023 L_postcing
1010 L_isthmuscing
1035 L_insula
1009 L_inferiortemporal
1033 L_temporalpole
2015 R_middletemporal
2002 R_caudantcing
2026 R_rostantcing
2023 R_postcing
2010 R_isthmuscing
2035 R_insula
2009 R_inferiortemporal
2033 R_temporalpole

Braak 5 and 6 composite region (Braak56):

Braak 5

1028 L_superior_frontal
1012 L_lateral_orbitofrontal
1014 L_medial_orbitofrontal
1032 L_frontal_pole
1003 L_caudal_middle_frontal
1027 L_rostral_middle_frontal
1018 L_pars_opercularis

1019 L_pars_orbitalis
1020 L_pars_triangularis
1011 L_lateraloccipital
1031 L_parietalsupramarginal
1008 L_parietalinferior
1030 L_superiortemporal
1029 L_parietalsuperior
1025 L_precuneus
1001 L_bankSuperiorTemporalSulcus
1034 L_tranvtemp
2028 R_superior_frontal
2012 R_lateral_orbitofrontal
2014 R_medial_orbitofrontal
2032 R_frontal_pole
2003 R_caudal_middle_frontal
2027 R_rostral_middle_frontal
2018 R_pars_opercularis
2019 R_pars_orbitalis
2020 R_pars_triangularis
2011 R_lateraloccipital
2031 R_parietalsupramarginal
2008 R_parietalinferior
2030 R_superiortemporal
2029 R_parietalsuperior
2025 R_precuneus
2001 R_bankSuperiorTemporalSulcus
2034 R_tranvtemp

Braak 6

1021 L_pericalcarine
1022 L_postcentral
1005 L_cuneus
1024 L_precentral
1017 L_paracentral
2021 R_pericalcarine
2022 R_postcentral
2005 R_cuneus
2024 R_precentral
2017 R_paracentral

Meta-temporal ROI [8]

18	L_amygdala
1006	L_entorhinal
1007	L_fusiform
1009	L_inferiortemporal
1015	L_middletemporal
54	R_amygdala
2006	R_entorhinal
2007	R_fusiform
2009	R_inferiortemporal
2015	R_middletemporal

Cerebellar Gray Matter

8	Left-Cerebellum-Cortex
47	Right-Cerebellum-Cortex

Eroded subcortical WM

This region is eroded by smoothing the WM mask by 8mm^3 FWHM, binarizing with a threshold of 0.7, and restricting the resulting mask to voxels labeled as WM.

2	Left-Cerebral-White-Matter
41	Right-Cerebral-White-Matter

PVC input regions

All Braak regions listed above

Other non-Braak-related regions used as PVC input

31	Left-choroid-plexus
63	Right-choroid-plexus
28	Left-VentralDC
30	Left-vessel
60	Right-VentralDC
62	Right-vessel
77	WM-hypointensities
80	non-WM-hypointensities
85	Optic-Chiasm
1000	ctx-lh-unknown
1004	ctx-lh-corpuscallosum
2000	ctx-rh-unknown
2004	ctx-rh-corpuscallosum

Not included in PVC model (set to zero). Note that bone, soft tissue, and CSF outside the brain are omitted and are all implicitly set to zero [2]

4 Left-Lateral-Ventricle
5 Left-Inf-Lat-Vent
14 3rd-Ventricle
15 4th-Ventricle
24 CSF
43 Right-Lateral-Ventricle
44 Right-Inf-Lat-Vent
72 5th-Ventricle

SUIT and FS ROI numbers used for Inferior Cerebellar Gray definition [7]

This region is defined by an intersection between the SUIT inferior cerebellar and the freesurfer cerebellar gray matter masks, excluding the SUIT superior cerebellar mask.

Inferior cerebellar inclusion mask: SUIT codes 6, 8-28, 33, 34
Superior cerebellar exclusion mask (bilateral lobules I-VI): SUIT codes 1-5, 7
Freesurfer cerebellar gray matter: 8, 47

Dataset Information

This methods document applies to the following dataset(s) available from the ADNI repository:

Dataset Name	Date Submitted
UC Berkeley - AV1451 Analysis [ADNI1,GO,2,3]	15 November 2021

References

1. Baker, S.L., et al., *Reference Tissue-Based Kinetic Evaluation of 18F-AV-1451 for Tau Imaging.* J Nucl Med, 2017. 58(2): p. 332-338.
2. Baker, S.L., A. Maass, and W.J. Jagust, *Considerations and code for partial volume correcting [(18)F]-AV-1451 tau PET data.* Data Brief, 2017. 15: p. 648-657.
3. Maass, A., et al., *Comparison of multiple tau-PET measures as biomarkers in aging and Alzheimer's disease.* Neuroimage, 2017. 157: p. 448-463.
4. Scholl, M., et al., *PET Imaging of Tau Deposition in the Aging Human Brain.* Neuron, 2016. 89(5): p. 971-982.

5. Braak, H. and E. Braak, *Neuropathological stageing of Alzheimer-related changes.* Acta Neuropathol, 1991. 82(4): p. 239-59.
6. Rousset, O.G., Y. Ma, and A.C. Evans, *Correction for partial volume effects in PET: principle and validation.* J Nucl Med, 1998. 39(5): p. 904-11.
7. Diedrichsen, J., *A spatially unbiased atlas template of the human cerebellum.* Neuroimage, 2006. 33(1): p. 127-38.
8. Jack CR Jr , Wiste HJ, Weigand SD, Therneau TM, Lowe VJ, Knopman DS, et al. *Defining imaging biomarker cut points for brain aging and Alzheimer's disease.* Alzheimers & Dementia. *2017*; 13: 205–16.

About the Authors

This document was prepared by Susan Landau, PhD, Jia Qie Lee, and Alice E. Murphy, Helen Wills Neuroscience Institute. For more information please contact Susan at 510-486-4433 or by email at slandau@berkeley.edu.